Fırat Üniversitesi Deneysel ve Hesaplamalı Mühendislik Dergisi

FUJECE

# Kuvvetli Rüzgar Etkisindeki Minarenin Göçme Mekanizmasının Simülasyonu

Taha Yasin ALTIOK[1*], Ali DEMİR[2]

[1,2]İnşaat Mühendisliği Bölümü, Mühendislik Fakültesi, Manisa Celal Bayar Üniversitesi, Manisa, Türkiye.
[1]taha.altiok@cbu.edu.tr, [2]ali.demir@cbu.edu.tr

Geliş Tarihi: 28.03.2024
Kabul Tarihi: 03.06.2024
Düzeltme Tarihi: 01.05.2024
doi: 10.62520/fujece.1460766
Araştırma Makalesi

Alıntı: T. Y. Altıok ve A. Demir,"Kuvvetli rüzgar etkisindeki minarenin göçme mekanizmasının simülasyonu", Fırat Üni. Deny. ve Hes. Müh. Derg., vol. 3, no 3, pp. 292-312, Ekim 2024.

**Öz**

Bu çalışmada, kuvvetli rüzgar etkisi altında göçen bir minarenin göçme mekanizması simüle edilerek, bu tür yapısal etkileşimlerin anlaşılması ve potansiyel riskli bölgelerin tespiti hedeflenmiştir. Rüzgar profilleri Eurocode ve Türk Standartları'na göre tanımlanmış ve Hesaplamalı Akışkanlar Dinamiği analizlerinde kullanılmıştır. Analizlerden elde edilen basınç ve emme gerilmeleri, Abaqus/Cae programında ilgili minare yüzeyine uygulanmış ve doğrusal olmayan sonlu eleman analizleri gerçekleştirilmiştir. Nümerik analizler sonucunda yer değiştirmeler, gerilmeler, plastik şekil değiştirmeler ve hasarlar elde edilmiş ve sonuçlar karşılaştırmalı olarak sunulmuştur. Her iki standartla elde edilen sonuçlar oldukça yakın olup, tepe yer değiştirmeleri İtalyan Yapı Kodu ve Eurocode 8'de belirtilen limit değerlerini aşmaktadır. Ayrıca, minarenin geçiş segmentindeki birçok ağ elemanı doğrusal olmayan sonlu eleman analizlerinde çekme gerilmeleri nedeniyle hasar görmüştür. Son olarak, minarenin göçme davranışı kullanılan yöntemlerle başarıyla simüle edilmiştir.

**Anahtar kelimeler:** Yığma, Göçme mekanizması, Rüzgar, Hasar analizleri, Hesaplamalı akışkanlar mekaniği

*Yazışılan yazar

İntihal Kontrol: Evet – Turnitin
Şikayet: fujece@firat.edu.tr

Firat University Journal of Experimental and Computational Engineering

# Simulation of the Collapse Mechanism of a Minaret under the Effect of Strong Wind

Taha Yasin ALTIOK[1*], Ali DEMİR[2]

[1,2]Department of Civil Engineering, Faculty of Engineering, Manisa Celal Bayar University, Manisa, Türkiye.
[1]taha.altiok@cbu.edu.tr, [2]ali.demir@cbu.edu.tr

Received: 28.03.2024
Accepted: 03.06.2024
Revision: 01.05.2024
doi: 10.62520/fujece.1460766
Research Article

Citation: T. Y. Altıok ve A. Demir, "Simulation of the collapse mechanism of a minaret under the effect of strong wind", Firat Univ. Jour.of Exper. and Comp. Eng., vol. 3, no 3, pp. 292-312, October 2024.

**Abstract**

In this study, the collapse mechanism of a destroyed minaret under strong wind influence was simulated to understand such structural interactions and identify potential risky regions. Wind profiles were defined according to Eurocode and Turkish Standards and were used in Computational Fluid Dynamics analyses. The pressure and suction stresses obtained with these wind analyses were applied on the minaret's surface with Abaqus and the nonlinear finite element analyses were performed. As a result of the numerical analyses, displacements, stresses, plastic strains, and damages were obtained and results were comparatively presented. The results obtained with both standards are quite close and top displacements exceed the limit value specified in the Italian Building Code and Eurocode 8. Besides, many mesh elements in the minaret's transition segment were damaged with tension stresses in nonlinear finite element analyses. Finally, the minaret's failure behaviour was successfully simulated with the used methods.

**Keywords:** Masonry, Failure mechanism, Wind, Damage analysis, Computational fluid mechanics

*Corresponding author

## 1. Introduction

The wind comprises numerous vortices of different sizes and rotational directions, transported within a prevailing air current that moves in relation to the surface of the Earth. The presence of these vortices imparts a turbulent character behaviour to the wind. The wind-induced response of structures encompasses static, stochastic, and resonant behaviors owing to turbulence and wake effects, vortex resonance, galloping, interference, divergence, and flutter. The wind loads depend on the wind strength, the topography of the terrain, and the interaction of wind and structures. Therefore, investigation of the wind effect on the structure and the relationship between the wind environment and movement is important to simulate a more realistic behaviour.

In certain regions, winds pose a greater threat to tall and slender structures like reinforced concrete (RC) or masonry minarets, RC chimneys, clock-lighting towers, silos, or turbine towers compared to earthquakes. Numerous studies in the literature have investigated these structures extensively. Chimneys may be subject to downwind gusts due to drag forces, as well as possible downwind eddy shedding. Reddy et al. [1] determined that the earthquake force exerted on the RC chimney in an area with a baseline wind velocity of 44 m/s is close to the wind load. Karaca and Türkeli [2] investigated the wind load and response of industrial RC chimneys by following the procedures of five different codes. They determined that the wind loads calculated according to the Eurocode-1 [3] are three to four times higher than the wind load values of other codes. So, they expressed that the Eurocode-1 was more reliable by determining the wind effects. They also determined that the effect of slender industrial RC chimneys on wind responses should be considered to perform a safe and economical design.

In recent times, structural engineers have placed more emphasis on investigating the performance of tall structures, considering various uncertainties for wind loads [4], [5], [6], [7], [8]. Li et al. [9] performed wind tunnel experiments to study the impact of wind on the Jin Mao Building, one of China's tallest structures, standing at 420.5 meters with 88 floors. The effectiveness of wind tunnel testing methods was verified by comparing full-scale measurements with wind tunnel test results. Additionally, an assessment of the building's performance under typhoon conditions was carried out. Merrick and Bitsuamlak [10] investigated the shape effects of wind triggering the response of tall buildings. Aly et al. [11] proposed a method to predict high-rise building responses to wind loads, which integrates lateral, crosswind, and torsional responses. Yang et al. [12] performed experiments on a high rise building model in hurricane like winds, finding that wind loads varied significantly based on the model's position relative to the center of the vortex. Heiza and Tayel [13] investigated the effects of earthquakes and winds on approximately 30 structures. They determined that the wind was more effective in tall buildings and the earthquake was more effective in low rise buildings. Kwon and Karaem [14] carried out a series of studies using 8 major regulations to develop a global standard within the scope of determining the wind effect. Ouyang and Spence [15] conducted probabilistic performance-based studies to estimate the damage to buildings exposed to extreme winds.

One of the structures most affected and damaged by the winds is the minarets. The architectural features of the minarets vary according to the construction age and material. While masonry materials demonstrate strong resistance to compressive stresses, they may encounter issues under tensile stresses. To address tensile stresses in historical minarets, masonry units (stone, brick) are interconnected both horizontally and vertically using clamps and dowels [16-17]. Most of the minarets in Turkey have been built as RC structures, recently [18]. Minarets are usually built by masters without any project [19]. After the 1999 earthquakes, it was announced that 80.9% of the 1176 mosques in Turkey didn’t have a building permit [19]. Many researchers have carried out experimental and numerical studies on minarets, especially involving earthquakes [16-17], [20-33]. Observations from the studies indicated that damages were primarily concentrated in the transition segment and upper part of the minarets [31-35].

Numerical examination methods refer to various calculation and simulation techniques used for structural analysis in engineering applications. These methods are commonly employed to understand the behaviors of complex structures, evaluate their performances, and optimize design processes. Common numerical examination methods include Finite Element Method (FEM), Finite Volume Method (FVM), Finite Difference Method (FDM), Finite Time Domain Method (FTDM), and Computational Fluid Dynamics

(CFD). These methods have different advantages and disadvantages depending on the engineering problems and their applications. In the context of structural behavior problems, Finite Element Method is generally preferred, while CFD methods are preferred for fluid mechanics. Wind effects can be assessed using either wind tunnel tests or Computational Fluid Dynamics (CFD) analysis. Physical wind tunnel tests are time consuming and costly. CFD modelling, which has recently been adopted in airflow studies in buildings, offers many advantages in evaluating wind performance. While structural models can be changed quickly in CFD analysis, design changes in physical studies require a lot of effort. CFD relies on the premise of a three-dimensional, fully turbulent, and incompressible flow regime. Both internal and external flows were simulated utilizing the standard k–epsilon turbulence model, a widely accepted technique within the realm of natural ventilation investigation [36-43]. In recent years, numerous studies have been conducted to determine the wind effects on minarets. Ural et al. [44] investigated the effects of dead load, wind load, and seismic load on an 800-year-old curved historical minaret in Aksaray and provided recommendations for restoration processes. Türkeli [2] studied the impacts of wind and earthquake loads on a 61-meter-high RC minaret. They recommended utilizing time history analysis to evaluate lateral loads in the design of RC minarets, emphasizing the importance of considering cross-section modifications. [45] explored the displacement mechanisms of minarets under dead load and wind load through various numerical studies. Based on the analysis results, insights were drawn regarding the errors made during the construction of minarets. . Reşatoğlu et al. [46] investigated the behaviour of some RC minarets in Cyprus under earthquake and wind loads calculated with various codes. They tried to determine the effective lateral load in minaret design by examining wind load and distributions, principal stresses, displacements, and base shear forces. Adam et al. [47] attempted to determine the behavior of a historical masonry minaret in Egypt under its own weight, wind, and seismic loads using nonlinear finite element analyses with static and dynamic loads. Türkeli [48] studied the behaviour of a historical masonry minaret under the wind and earthquake loads. In the study, the wind was more dominant in the behaviour of the minaret. It was expressed that the main cause of the failure is the tensile and shear stress buildup on the cylindrical body and the transition segment. Pouraminian [49] examined the behavior of a historical brick minaret in Iran, with a height of 16.11 meters, against wind and seismic loads. According to the results, the minaret was found to be at a slight risk of damage under seismic loading and safe even under strong wind effects. Al-Zuhairi et al. [50] conducted finite element analyses on a historical masonry minaret, considering wind and self-weight loads. They concluded that the minaret exhibited sufficient resistance against principal stresses occurring only when both self-weight and wind load up to 120 km/h were acting together. Awad and Desouki [51] investigated the potential use of mosque minarets as solar chimneys in hot and arid regions. Through laboratory tests and CFD simulations, they concluded that traditional mosque minarets could serve as a viable and sustainable option for passive cooling in hot climates. Masonry structures are divided into three groups based on the accuracy required for modeling with FEM: Detailed Micro Modeling, Simplified Micro Modeling, and Macro Modeling. In Detailed Micro Modeling, the properties of each material constituting the structure (stone, brick, mortar, etc.), such as compressive and tensile strength, Poisson's ratio, elasticity modulus, and shear modulus, are individually inputted into the system, and separate modeling is performed. Detailed Micro Modeling provides more realistic results than other modeling methods. However, it is more time-consuming during the solution phase compared to other methods. In Simplified Micro Modeling, the region where mortar is present is neglected, and modeling is done by enlarging the dimensions of the materials constituting the masonry unit by half the size of the neglected mortar layer. Masonry units are separated from each other by interface lines, and joint interface lines are defined separately. It is assumed that cracks occur on these surfaces. In Macro Modeling, the structural element subjected to homogenization is considered as a composite material. Especially in nonlinear analyses, the increase in the number of unknowns and the stiffness matrix of large-sized systems prolong the solution time. In such cases, the homogenization technique ensures that the brick-stone and mortar, which constitute the wall structure of a masonry structure, are entered as a single material. This approach not only ensures realistic modeling and analysis of the structure but also provides significant time savings in the modeling and analysis stages.

In the current literature, research on the seismic effects on minaret-type structures is commonly conducted. However, studies regarding the influence of wind are seldom undertaken. In these studies, the surrounding structures of the wind-affected building are often being neglected, and the impact of neighboring structures on wind flow are not taken into account. This study, however, focuses on investigating the wind effects on delicate, tall, and slender structures, taking into consideration the

presence of surrounding buildings. In this context, the behaviour of a concrete minaret collapsed with a wind effect is simulated. A wind profile is created using TS 498 [52] and Eurocode-1 [3]. CFD numerical simulation analyses are performed using the wind profiles with the RWIND program [53]. In these analyses, environmental factors are considered by modelling other structures around the minaret. Nonlinear Static/General analyses are carried out by applying the wind's pressure and suction stresses on the minaret's surfaces modelled in the Abaqus/Cae [54]. Consequently, the minaret's failure mechanism is estimated by considering the displacements, stresses, and damages. Considering the results obtained, this study offers important ideas for predicting the behaviour of thin and tall structures that are fragile against dynamic effects under the influence of wind. In addition, it gives more realistic results by considering the effect of a collapsed minaret on the wind flow in the surrounding structures.

## 2. Wind damages of minarets

The wind is an important dynamic effect, especially for slender structures. Turkey's coastal regions have a high potential to face severe windstorms. The strong winds destroyed many minarets in the past. In 2002, during a storm, the minaret of Ebubekir Sıddık Mosque in Ankara-Kayaş collapsed, leading to the death of two individuals and injuring five others (Figure 1a) [55]. On February 27, 2002, the five minarets collapsed, and the four minarets got damaged because of a wind speed of 96 km/h in Mersin-Erdemli (Figure 1b) [56]. On February 9, 2003, another minaret collapsed due to the wind speed of 100 km/h (Figure 1c) [57]. Two 15 m high minarets of the Ulu Mosque in Kahramanmaraş collapsed in 2005 during a 60 km/h windstorm and one person got injured (Figure 1d) [58]. The stone minaret of the 22-year-old Kurtuluş Mosque collapsed due to the strong wind that occurred in Kırıkkale in 2010 (Figure 1e) [59]. In February 2015, the minaret of Şafak Mosque in İzmir collapsed during a strong windstorm with a maximum wind speed of 90 km/h (Figure 1f) [60]. In Ordu Ulubey, the longest minaret in the city with a length of 57 m collapsed due to the strong wind effect in 2016 (Figure 1g) [61]. Due to the wind in Niğde, a minaret collapsed from the transition zone in January 2021 (Figure 1h) [62]. In Aydın Nazilli, the upper part and spire of a minaret collapsed due to the wind with an average speed of 70 km/h in October 2021 (Figure 1i) [63].


**Figure 1.** Minarets damaged by wind, (a) Ebubekir Sıddık Mosque/Ankara-Kayaş, (b)-(c) Mersin-Erdemli, (d) Ulu Mosque/Kahramanmaraş, (e) Kurtuluş Mosque/Kırıkkale, (f) Şafak Mosque/İzmir, (g) Ordu-Ulubey, (h) Niğde, (i) Aydın/Nazilli


**Figure 1.** Minarets damaged by wind, (a) Ebubekir Sıddık Mosque/Ankara-Kayaş, (b)-(c) Mersin-Erdemli, (d) Ulu Mosque/Kahramanmaraş, (e) Kurtuluş Mosque/Kırıkkale, (f) Şafak Mosque/İzmir, (g) Ordu-Ulubey, (h) Niğde, (i) Aydın/Nazilli (Continue)

## 3. General Properties of the Collapsed Minaret

### 3.1. Geometrical Properties

The minaret of the Industry mosque was built in Manisa in 1989. The minaret consists of a boot, transition segment, cylindrical body, two balconies, upper part, spire, and end ornament parts. (Figure 2a-2b). It was built using concrete blocks and binder mortar as the building material. No steel element was used in its construction. There is a core body staircase inside the minaret. The average height of the stairs is 20 cm. The total height of the minaret is 33.20 m. The pedestal dimensions of the minaret are 2.27 x 2.27 $m^2$. Its geometric properties are given in Figure 2c.

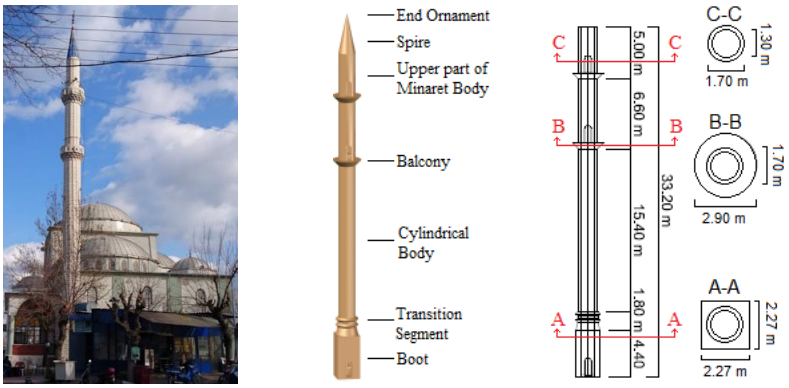


**Figure 2.** The parts and geometric features of the minaret. (a) Industry mosque and minaret, (b) Parts and (c) Geometrical properties

### 3.2. Damage Survey

Many buildings got damaged due to the windstorm that occurred in Manisa on January 27, 2021. The most striking of these damages was the failure of Industry Mosque's minaret. According to the information obtained by the Provincial Meteorology Directorate, the wind's maximum speed was 25.8 m/s (92.9 km/h). It was observed that there was a double row concrete block in the transition segment of the minaret. At the same time, the minaret had 2 balconies and a tall body. It was foreseen that the minaret collapsed by the influence of the stresses accumulated in the transition segment. The photographs of the minaret before and after the collapse are presented in Figure 3.

**Figure 3.** Before and after the collapse of the minaret of Industry Mosque

## 3.3. Materials

Following the collapse of the minaret due to wind, various tests were conducted on samples extracted from its concrete blocks and mortar material. Compression tests were administered, yielding an average compressive strength ($f_b$) of 6.30 MPa for the concrete blocks and 3.36 MPa for the mortar sample. According to the Turkish Building Earthquake Code-2018 (TBEC-2018) [64], the compressive strength ($f_K$) of the masonry wall is determined as 3.34 MPa. Based on TBEC-2018, the modulus of elasticity of the masonry wall ($E_{duv}$) can be determined as 750 times $f_K$. Consequently, the modulus of elasticity is calculated as 2504.3 MPa.

## 4. Wind Analyses

In this study, CFD analyzes of a minaret that collapsed due to the wind were carried out using wind profiles calculated according to TS 498 and Eurocode-1 regulations. Other structures around the minaret were also included in the modeling. Pressure and suction values on the minaret surface under the influence of the wind were obtained and applied to the relevant surfaces of the minaret modeled in ABAQUS. The obtained results are presented comparatively and the collapse mechanism of the minaret is simulated. The flow chart of the study is given in Figure 4.

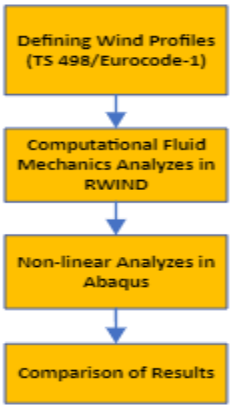


**Figure 4.** The flow chart of the study

## 4.1. Wind Loads According to Eurocode-1 and TS 498

Due to the speed and mass of the moving air, if an object with a fixed position comes in front of the air with kinetic energy, its flow will either stop or its direction will be deflected. The magnitude of wind pressure exerted on any surface of an object is subject to variation based on several factors, including the object's geometry, wind direction, wind speed, and air density. Obstacles present on the ground surface diminish wind velocity, with speed escalating proportionally with height. Wind velocity attains its peak value at an elevation known as the gradient height (Table 1).

**Table 1.** Wind speed and suction stresses (TS 498)

| Height (h) (m) | Wind speed (n) m/s | km/h | Suction (q) (kN/m$^2$) |
|---|---|---|---|
| 0-8 | 28 | 100 | 0.5 |
| 9-20 | 36 | 130 | 0.8 |
| 21-100 | 42 | 150 | 1.1 |
| > 100 | 46 | 165 | 1.3 |

The minaret's wind profiles were obtained according to Eurocode-1 and TS 498 standards in this study. TS 498 and Eurocode-1 are among the most common standards used for wind load designing in Turkey. TS 498 is generally used for load bearing systems and facade elements. Some international standards and regulations provide more detail. TS 498 can be used regardless of the structural carrier system (RC, steel, masonry, wood). In TS 498, the wind pressure ($w$), which does not directly affect the building carrier system, but directly affects the unit area on the upper surface of the building, is calculated with equation 1. ($q$) is the wind pressure acting perpendicular to the surface, and $C_p$ is the suction coefficient determined for the surface, depending on the various blowing directions.

$$w = C_p \times q \tag{1}$$

In Eurocode-1, some formulations express the wind speed variation and turbulence intensities depending on the height. $V_{mz}$ represents the wind speed at height $z$ and is calculated as shown in equation 2.

$$V_m(z) = c_r(z) \times c_0(z) \times V_b \tag{2}$$

$V_b$ is the basic wind velocity and is calculated as in equation 3.

$$V_b = c_{dir} \times c_{season} \times V_{b,0} \tag{3}$$

Equation 3 introduces the directional factor, $c_{dir}$, where $V_{b,0}$ represents the fundamental value of the basic wind velocity, and $c_{season}$ denotes the seasonal factor. According to the Eurocode-1, both the direction ($c_{dir}$) and season ($c_{season}$) factors can be assumed as 1.00.

In equation 2, $c_r(z)$ is the roughness factor and $c_o(z)$ is the orography factor. It started in the Eurocode-1 that it is appropriate to take the Orography factor ($c_o(z)$) as 1. The roughness factor ($c_r(z)$) is calculated as in equation 4.

$$c_r(z) = k_r \times \ln\left(\frac{z}{z_0}\right) \qquad z_{min} \le z \le z_{max} \qquad (4)$$
$$c_r(z) = c_r(z_{min}) \qquad z \le z_{min}$$

In equation 3, kr is the terrain factor and can be calculated using equation 5.

$$k_r = 0.19\left(\frac{z_0}{z_{0.11}}\right)^{0.07} \qquad (5)$$

$z_{min}$ is the lowest height, $z_0$ is the roughness length and $z_{max}$ is the highest height depending on the terrain category. $z_{min}$, $z_0$ and $z_{max}$ values are determined as 5 m, 0.3 m and 200 m, respectively. The obtained results are presented in Table 2.

**Table 2.** Roughness factor, orography factor, basic wind velocity and wind velocity values depending on height

| No | Height from ground | $c_r(z)$ | $c_0(z)$ | $V_b$ | $V_m(z)$ |
|---|---|---|---|---|---|
| 1 | 0-4.4 | 0.59092 | 1 | 19.76 | 11.6765792 |
| 2 | 4.4-6.2 | 0.66638 | 1 | 22.28 | 14.8469464 |
| 3 | 6.2-21.6 | 0.94094 | 1 | 31.47 | 29.6113818 |
| 4 | 21.6-27.6 | 0.99484 | 1 | 33.27 | 33.0983268 |
| 5 | 27.6-33.2 | 1.03554 | 1 | 34.63 | 35.8607502 |

According to Eurocode-1, the wind turbulence intensity ($l_v$) can be calculated using equation 6. The obtained values are given in Table 3.

$$l_v(z) = \frac{k_l}{c_o(z) \times \ln\left(\frac{z}{z_0}\right)} \qquad z_{min} \le z \le z_{max} \qquad (6)$$
$$l_v(z) = l_v(z_{min}) \qquad z \le z_{min}$$

In equation 6, specifies the turbulence coefficient, denoted as $k_l$, with a recommended value of 1.0. As for the orography coefficient $c_0(z)$, a value of 1.0 is suggested when there is no discernible increase in velocity induced by turbulence on the terrain (Table 3).

**Table 3.** Wind turbulence intensities depending on height

| No | Height from ground | $l_v(z)$ |
|---|---|---|
| 1 | 0-4.4 | 0.372 |
| 2 | 4.4-6.2 | 0.33 |
| 3 | 6.2-21.6 | 0.234 |
| 4 | 21.6-27.6 | 0.221 |
| 5 | 27.6-33.2 | 0.212 |

## 4.2. Numerical Simulation of the Minaret's Wind Flow

For the structures, determining the wind effect is quite complex. In such cases, one possible solution is to test the relevant buildings in a wind tunnel. This method is both expensive and time consuming. Another method is to use the programs that can perform CFD simulations. RWIND software, which can perform CFD simulations, is used in the wind analysis of the minaret. RWIND Simulation is a software application designed for conducting numerical simulations of wind flow, akin to a digital wind tunnel, particularly around buildings or other structures. Its primary function encompasses generating wind loads, representing the forces exerted on these objects due to wind effects. The wind speed profiles and turbulence intensities, which are the main parameters in the analyses, are determined according to TS 498 and Eurocode-1. The structure and surrounding conditions (structures, vehicles, trees, mountains, seas, etc.) are crucial to realistically determining the wind's effect on the structure. So, numerical models are created by considering the structures that can change the wind effect around the minaret. Satellite views of the minaret and its surrounding structures are presented in Figure 5, and a 3D model of the minaret and its surrounding structures are presented in Figure 6a. After the minaret collapsed, the effective wind direction is determined with on-site investigations. The wind angle is considered as 450 in all analyses. Besides, the dimensions of the wind tunnel, and the mesh sizes of the minaret and surrounding structures are all taken equally. In CFD modelling, mesh type and size greatly affect the accuracy of the results. The grid has been modified and improved according to the wind area. The mesh element size was gradually increased in a smooth manner to effectively resolve sections exhibiting high gradient mesh, thereby enhancing the accuracy of the velocity field results. Grid sensitivity analysis was employed to validate both the programming and computational functionality of the computational model. The grid, number of nodes, and elements were calibrated until the posterior prediction error between the calculation iterations and the posterior error indicator became negligible. The applied boundary conditions were kept constant throughout the simulation to ensure a precise comparison of the posterior error estimation. As a result of the studies, the mesh size was determined as 0.997 m (mesh density 40%). Accordingly, the minaret and its surroundings have 666703 meshes and 780184 nodes. The main input parameters of the simulation are kinematic viscosity 15x10-6 $m^2/s$ and air density 1.25 $kg/m^3$ (Eurocode-1). Figure 6b is used to clearly determine the pressure and suction effects on the minaret. The wind flow chart that occurred during the analysis is presented in Figure 6c.


**Figure 5.** Satellite view of the minaret and its surrounding

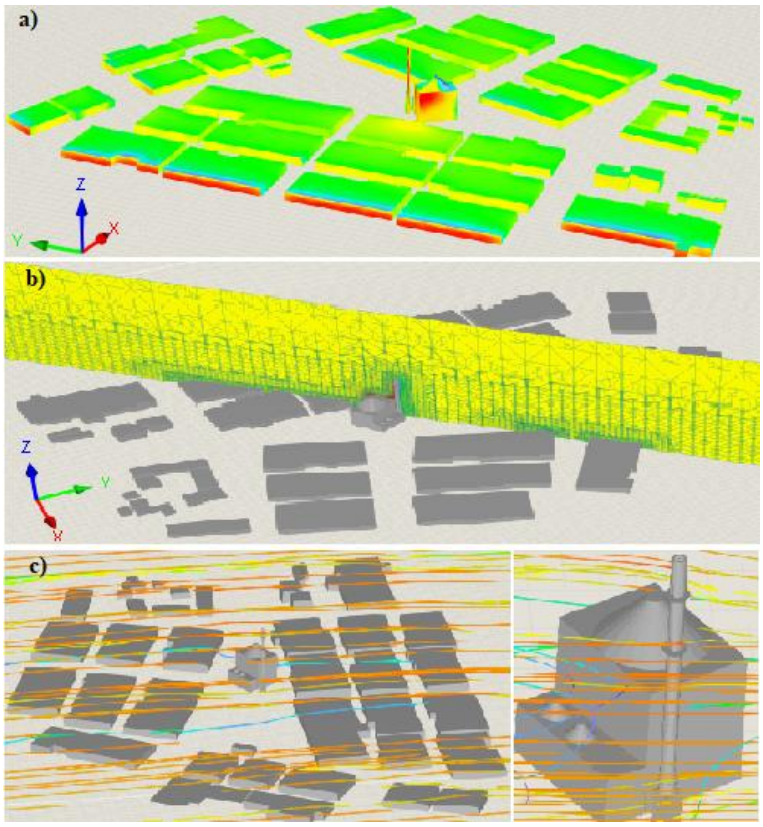


**Figure 6.** General view of wind flow and wind pressure effect on the surface of structures

## 4.3. Wind's Pressure and Suction Values

The wind profiles made with TS 498 and Eurocode-1 are shown in Figure 7. The pressure and suction values obtained in Figures 6b and 6c are presented in Figure 8. In all analyses, the suction effect occurs on the front surface, and the pressure effect occurs on the back surface of the minaret. Positive pressure is defined as the force directed towards the surface, while negative pressure, or suction, denotes the force moving away from the surface. According to the results, it is determined that the TS 498 has a more compelling effect than the Eurocode-1. The maximum pressure on the back surface of the minaret is 862.9 Pa and 777 Pa in TS 498 and Eurocode-1, respectively. The maximum suction on the front surface of the minaret is 1477.5 Pa in TS 498 and 951.3 Pa in Eurocode-1. Although the pressure and suction values are constant in the straight parts, those in varying cross-sections suddenly change. Obtained with the wind analyses, the pressure and suction values are presented in Figure 9. It is determined that the pressure and suction values increase with the height. According to the results, the wind effect reaches the highest value in the upper part of the minaret. This effect considerably increases the overturning moment. When considering the pressure and suction values calculated with TS 498 and Eurocode-1, close results are obtained.

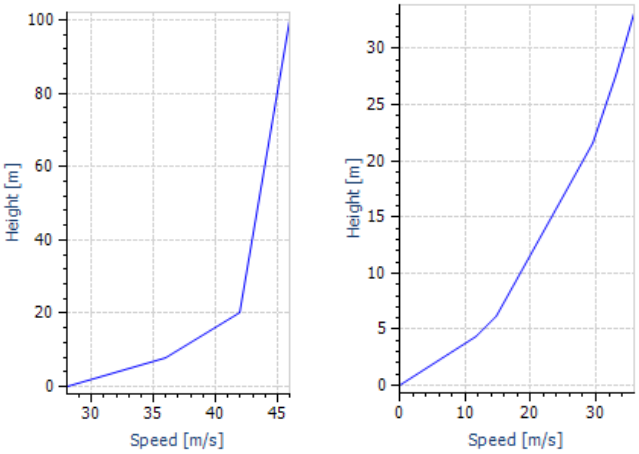


(a) (b)

**Figure 7.** Wind profiles. (a) TS 498, (b) Eurocode-1

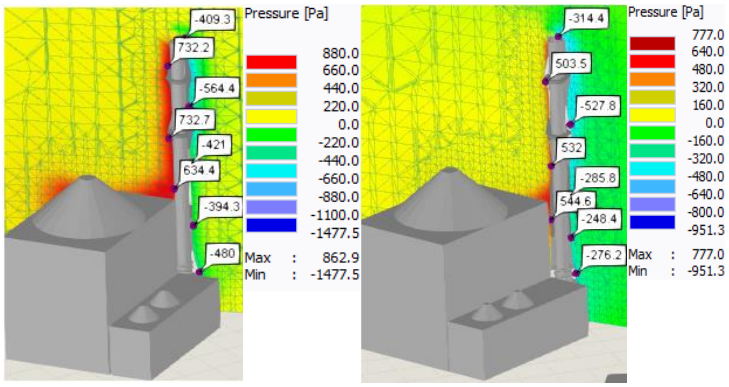


(a) (b)

**Figure 8.** Pressure and suction formed on the minaret surface. (a) TS 498, (b) Eurocode-1

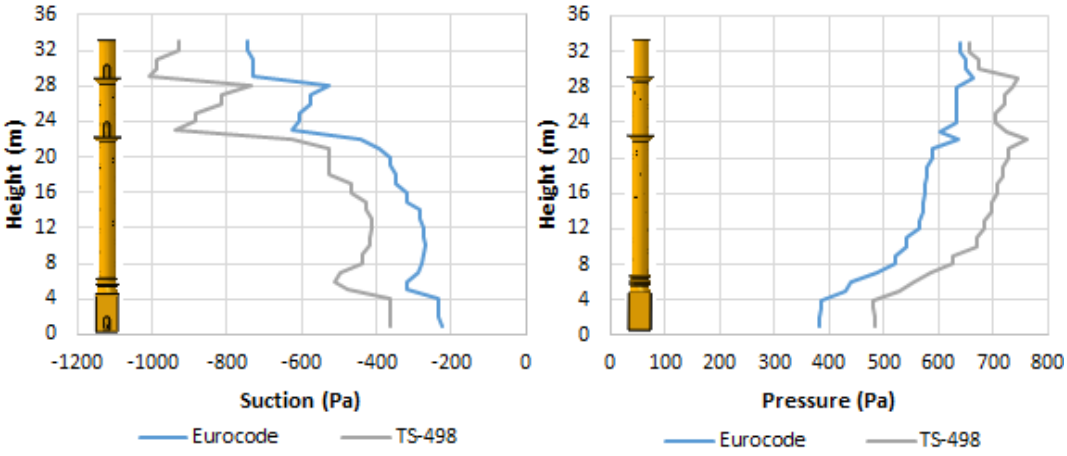


**Figure 9.** Pressure and suction values occurred on minaret's surfaces

## 5. Nonlinear FE Analyses

As a result of the wind analyses performed with RWIND software, the pressure and suction values on the minaret surface are determined. The pressure and suction values obtained with the wind analyses are applied on the relevant surface of the minaret FE model in the Abaqus program. The large geometric dimensions of the minaret and the high number of mesh elements obtained in convergence analyses increase the analysis

time. A composite material model representing the common material properties of the masonry units and mortar is selected for macro modelling. This method is frequently preferred for modeling large systems due to its significant reduction in computational time. In this study, the relevant minaret is modeled using the macro modeling technique. For this purpose, load surfaces are created on each of the minaret's back and front surfaces, with one-meter intervals on the right and left surfaces. Pressure and suction stresses are applied on these load surfaces and nonlinear Static/General analyses are performed (Figure 10b). The minaret is not adjacent to the mosque. All degrees of freedom on the foundation surface of the minaret were accepted as fixed support under initial boundary conditions (Figure 10a). The convergence analyses are performed to create a more realistic and consistent FE model (as shown in Figure 11). The Convergence graph means approaching a point, a limit, with the gap in between getting smaller, but without intersecting. The mesh size, which directly affects the analysis time and results, is determined by the analyzes made to obtain this graph. In the analyses, the optimum mesh size is determined as 0.35 m. In total, the FE model has 29412 quadratic tetrahedral (C3D10) mesh elements. Mesh properties are kept the same in all analyses.

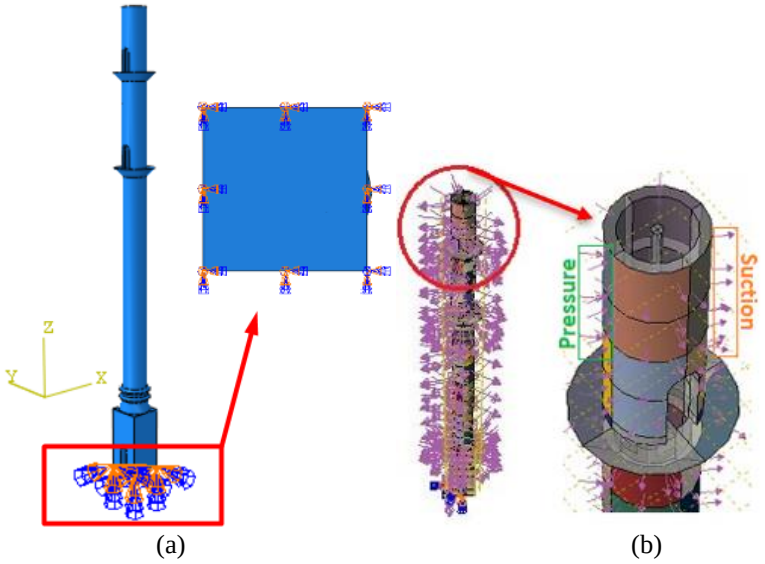


**Figure 10.** (a) Boundary conditions, (b) Applying pressure and suction stresses to relevant surfaces in Abaqus

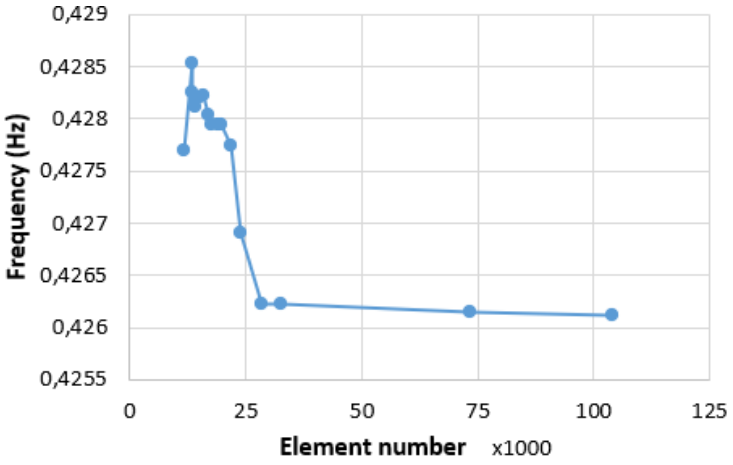


**Figure 11.** Convergence analysis of the minaret

The natural frequencies corresponding to the first three modes and their corresponding mode shapes obtained through finite element analysis under the initial mechanical parameters and boundary conditions of the minaret are presented in Figure 12. The first two modes represent bending modes in both the x and y directions, while the third mode represents a torsional mode.

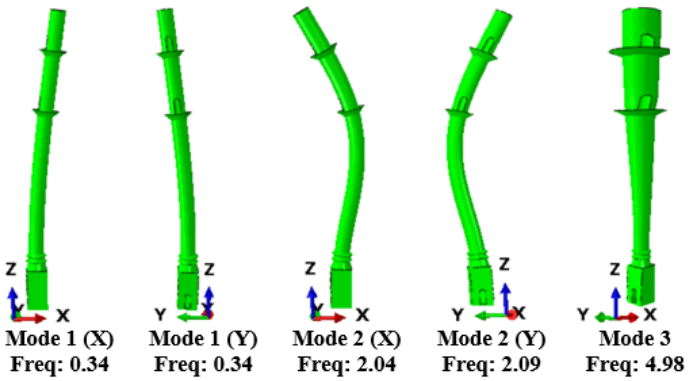


**Figure 12.** Mode shapes and natural frequencies of the minaret

## 5.1. Concrete Damage Plasticity Model

In this study, Concrete Damage Plasticity Model (CDP) was chosen to characterize the inelastic response of concrete in Abaqus. Even though the CDP material model was initially designed to capture the plastic behavior of concrete [65-66], the CDP model has also demonstrated its applicability to masonry structures [67-69]. In existing literature, there is a widespread use of the CDP material model to describe the plastic behavior of masonry structures [32-33], [68-71]. The CDP model integrated into Abaqus encompasses the plastic, compressive, and tensile behaviors exhibited by concrete. In this investigation, the plastic behavior of the concrete minaret was determined based on the values outlined in Table 4.

**Table 4.** Material parameters

| Dilation angle | Eccentricity | $f_{bo}/f_{co}$ | K | Viscosity |
|---|---|---|---|---|
| $35^O$ | 0.1 | 1.16 | 0.667 | 0.0058 |

With the initial modulus of elasticity denoted as $E_o$, the stress-strain relationship under axial compressive and tensile loads is obtained as in equations 7-8.

$$\sigma_c = (1 - d_c)E_0\left(\varepsilon_c - \varepsilon_c^{-pl}\right) \quad (7)$$

$$\sigma_t = (1 - d_t)E_0\left(\varepsilon_t - \varepsilon_t^{-p_l}\right) \quad (8)$$

Here, $E_0$ represents the initial modulus of elasticity. $\sigma_c$ ($\sigma_t$) denotes the uniaxial compressive (tensile) stress, while $\varepsilon_c$ ($\varepsilon_t$) stands for the total strain experienced under compressive and tensile conditions, respectively. $\varepsilon_c$-$p_l$ ($\varepsilon_t$-$p_l$) represents the equivalent plastic strain under such conditions. Additionally, $d_c$ and $d_t$ are the damage parameters associated with compressive and tensile stresses, respectively.

The materials constituting masonry structures typically exhibit low tensile strengths but high compressive strengths. It is widely acknowledged in the literature that the primary cause of collapse in such structures is attributed to tensile stresses [32, 33, 72]. Various models for tensile stiffness have been proposed [73]. In this study, the tensile stiffness model proposed by Nayal and Rasheed [73], subsequently modified by Wahalathantri et al. [74], was employed (Figure 13). This model bears resemblance to the tensile stiffness model utilized in the CDP model in Abaqus [54]. Its foundation lies in the homogenized stress-strain diagram formulated by Gilbert and Warner [75], which accurately captures the response induced by primary and secondary cracking phenomena through two descending segments of the tensile stress-strain curve [75]. In this adapted model, the sole alteration was the adjustment of the sudden decline in the tensile stress-strain curve at a critical strain $\varepsilon_{cr}$, from the ultimate stress σt0 to $0.77\sigma_t0$, as opposed to the previously utilized $0.80\sigma_to$. The ultimate tensile strength of concrete can be estimated using equation 9 proposed by Genikomsu and Polak [76]. The values specified in Table 5 were employed in the static/general analyses of the minaret under pressure loading.

$$f_t' = 0.33\sqrt{f_c'}(\text{MPa}) \quad (9)$$

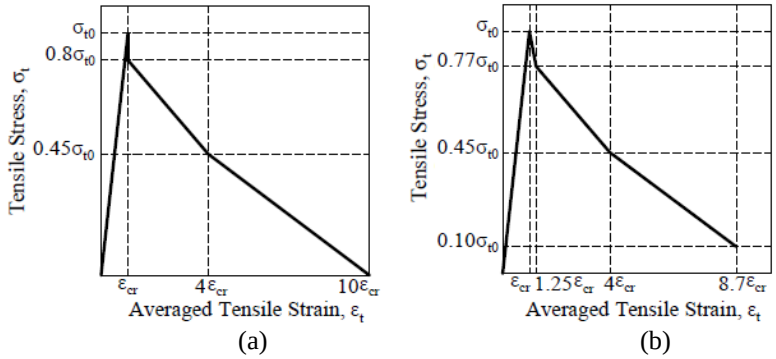


**Figure 13.** Tensile stiffness models: (a) Averaged tensile strain [73] (b)modified averaged tensile strain [74]

**Table 5.** The stress-strain curve values and scalar damage parameters for tensile behavior in masonry units

| Tensile behavior | | | |
|---|---|---|---|
| Yield stress (MPa) | Cracking strain | Damage | Cracking strain |
| 0.334 | 0 | 0 | 0 |
| 0.236531 | 0.000982 | 0.291824 | 0.000982 |
| 0.053322 | 0.007856 | 0.893603 | 0.000516 |
| 0.035554 | 0.010803 | 0.938922 | 0.013749 |

## 6. Results and Discussion

The pressure and suction stresses obtained with the wind analyses are applied on the minaret surfaces in Abaqus/Cae. To apply the stresses on the minaret surface, the FE model is divided into 2 parts horizontally and vertically at intervals of 1 m. The stresses are applied to the minaret surface in the horizontal direction. The pressure values on the minaret surface do not follow a uniform distribution. In nonlinear FE analyses, the mesh elements subjected to plastic deformation and tensile stresses, and displacements are determined. The top displacements of the minaret are presented in Figure 14. In the Italian Building Code [77] and Eurocode 8-Part-3 [78], if top displacement exceeds 0.4% of the masonry structure's height, the structure can get damaged or collapse. Since the minaret is 33.2 m high, the collapse limit displacement is 0.132 m according to the Italian Building Code and Eurocode 8-Part-3. This value is shown with a dashed red line in Figure 14. According to the results, the minaret's top displacement exceeds the limit value according to TS 498 and Eurocode-1. Figure 15 shows the displacement behaviour of the minaret.

Tension damages concentrate in the minaret's transition segment as shown in Figure 16. Many meshes get damaged more than 90%. It is understood that the minaret may collapse with the damages in the transition segment. The number of damaged and plastic elements according to both codes is quite similar (Figure 17). When the collapse mechanisms of masonry structures and especially tall and thin structures such as minarets are investigated, one of the most important reasons for their collapse is tensile stresses in the transition segment [72, 79, 80]. As a result of the damage analyses, the ratio of the elements damaged due to tensile stress to all elements is 0.85 in TS 498 and 0.84 in Eurocode-1. In addition, when the proportion of the number of plastic elements to all elements' number is investigated, it is 0.87 in both TS 498 and Eurocode-1.

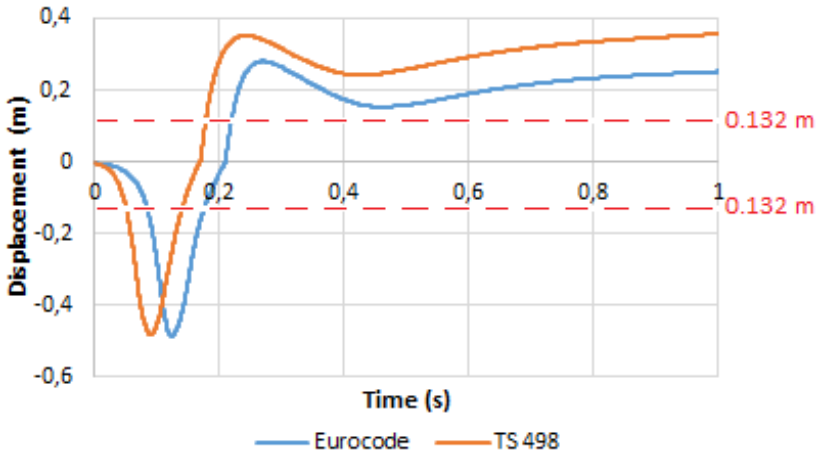


**Figure 14.** The displacements of the minaret's top

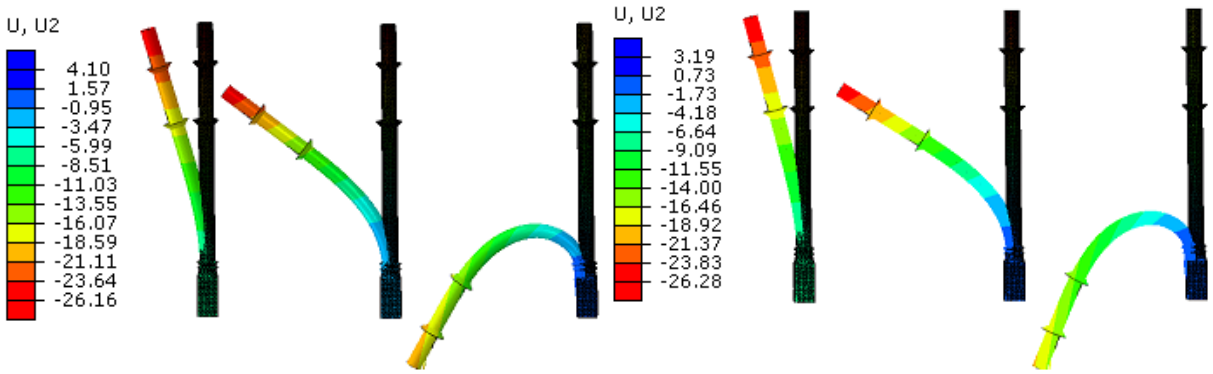


(a) TS 498 (b) Eurocode-1

**Figure 15.** The minaret's displacement behavior

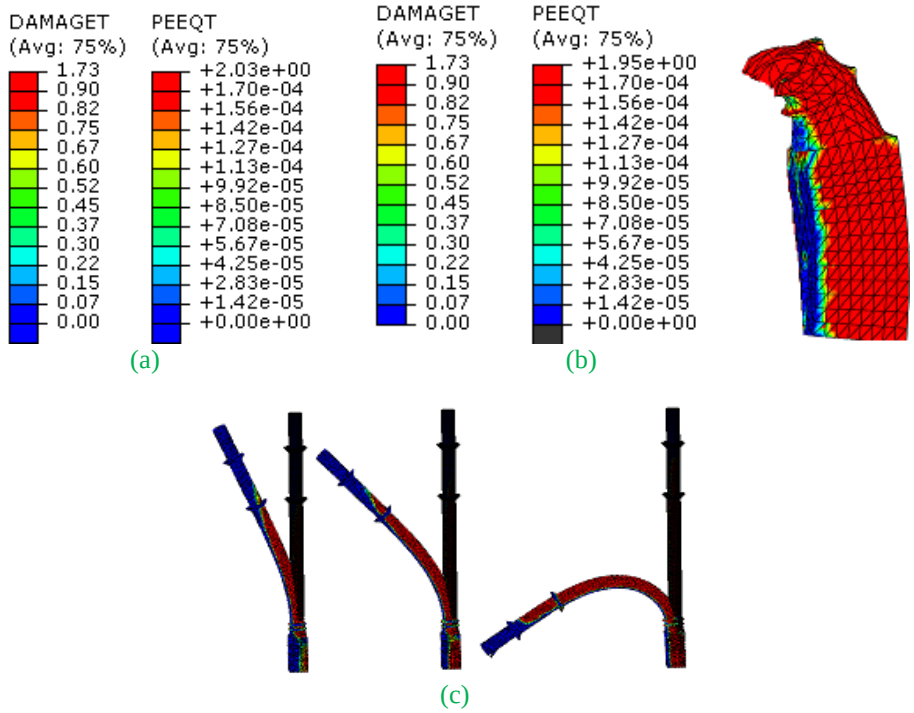


(a) (b)

(c)

**Figure 16.** Damaget and PEEQT values and damage distribution. (a) TS 498, (b) Eurocode-1, (c) Development of tensile damage and deformation of the minaret under the influence of stresses

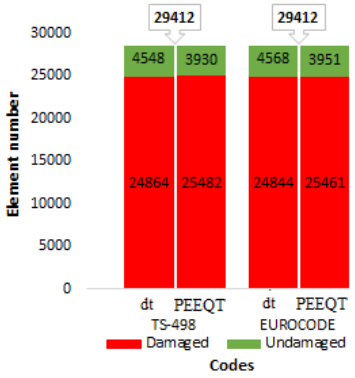


**Figure 17.** Number of damaged and undamaged elements

## 7. Conclusion

On January 27, 2021, a masonry minaret located in the western region of Turkey collapsed due to wind exposure with an average speed of 25.8 m/s. This study aims to conduct numerical analyses on the collapsed minaret and estimate its failure mechanism in accordance with TS 498 and Eurocode-1 standards, contributing to the literature in structural engineering. The numerical analyses entail two main stages. Firstly, Computational Fluid Dynamics (CFD) analyses are conducted using RWIND software to assess the wind flow around the minaret and its adjacent structures. The shape of the minaret and its surroundings significantly influence the wind flow patterns, hence necessitating the modeling of surrounding structures for comprehensive wind flow analyses with RWIND software. Subsequently, nonlinear analyses are carried out in Abaqus, incorporating pressure and suction effects obtained from the wind flow analyses to assess displacement and damage.

Evaluation of maximum pressure stresses on the minaret's rear surface reveals that TS 498 exceeds Eurocode-1 by 10%. Similarly, investigation into the maximum suction effects on the minaret's front surface indicates a 35.6% discrepancy between TS 498 and Eurocode-1. The observed top displacements surpass the limit values specified in the Italian Building Code and Eurocode 8-Part-3. Damage analysis demonstrates a close correlation between TS 498 and Eurocode-1, with an average consistency of 86% across both standards.

The simulation successfully identifies the failure mechanism of the minaret, attributing the collapse to accumulated tensile stresses in the transition segment. This underscores the importance of considering wind effects in conjunction with seismic loads for tall and slender structures. Furthermore, it is recommended to avoid geometric designs driven solely by architectural aesthetics, as such designs may compromise structural integrity.

## 8. Author Contribution Statement

In the conducted study, Author 1 contributed to the performance of finite element analyses, literature review, and obtaining results; while Author 2 contributed to the formation of ideas, examination of results, proofreading, and checking the article in terms of writing and content.

## 9. Ethics Committee Approval and Conflict of Interest

There is no need for an ethics committee approval in the prepared article. There is no conflict of interest with any person/institution in the prepared article.

## 10. References

[1] K. R. C. Reddy, O. R. Jaiswal, and P. N. Godbole, "Wind and earthquake analysis of tall RC chimneys," Int. J. Earth Sci. Eng., vol. 4, no. 6, pp. 508–511, 2011.
[2] Z. Karaca and E. Türkeli, "Determination and comparison of wind loads for industrial reinforced concrete chimneys," Struct. Des. Tall Spec. Build., vol. 21, no. 2, pp. 133–154, 2012.
[3] Eurocode-1, "Actions on Structures/General Actions, Part 1-4: Wind Actions," CEN/TC 250, Management Centre, Brussels, 2005.
[4] S. M. Spence and M. Gioffrè, "Large scale reliability-based design optimization of wind excited tall buildings," Probabilistic Eng. Mech., vol. 28, pp. 206–215, 2012.
[5] E. Bernardini, S. M. Spence, and A. Kareem, "A probabilistic approach for the full response estimation of tall buildings with 3D modes using the HFFB," Struct. Saf., vol. 44, pp. 91–101, 2013.
[6] D. T. Resio, J. L. Irish, J. J. Westerink, and N. J. Powell, "The effect of uncertainty on estimates of hurricane surge hazards," Nat. Hazards, vol. 66, no. 3, pp. 1443–1459, 2013.
[7] L. Caracoglia, "A stochastic model for examining along-wind loading uncertainty and intervention costs due to wind-induced damage on tall buildings," Eng. Struct., vol. 78, pp. 121–132, 2014.
[8] A. Suryawanshi and D. Ghosh, "Wind speed prediction using spatio-temporal covariance," Nat. Hazards, vol. 75, no. 2, pp. 1435–1449, 2015.
[9] Q. S. Li, Y. Q. Xiao, J. Y. Fu, and Z. N. Li, "Full-scale measurements of wind effects on the Jin Mao building," J. Wind Eng. Ind. Aerodyn., vol. 95, no. 6, pp. 445–466, 2007.
[10] R. Merrick and G. Bitsuamlak, "Shape effects on the wind-induced response of high-rise buildings," J. Wind Eng., vol. 6, no. 2, pp. 1–18, 2009.
[11] A. M. Aly, A. Zasso, and F. Resta, "Tall buildings under multidirectional winds: response prediction and reduction," Wind Tunn. Exp. Fluid Dyn. Res., p. 301, 2011.
[12] Z. Yang, P. Sarkar, and H. Hu, "An experimental study of a high-rise building model in tornado-like winds," J. Fluids Struct., vol. 27, no. 4, pp. 471–486, 2011.
[13] K. M. Heiza and M. A. Tayel, "Comparative study of the effects of wind and earthquake loads on high-rise buildings," Concr. Res. Lett., vol. 3, no. 1, pp. 386–405, 2012.
[14] D. K. Kwon and A. Kareem, "Comparative study of major international wind codes and standards for wind effects on tall buildings," Eng. Struct., vol. 51, pp. 23–35, 2013.
[15] Z. Ouyang and S. M. Spence, "Performance-based wind-induced structural and envelope damage assessment of engineered buildings through nonlinear dynamic analysis," J. Wind Eng. Ind. Aerodyn., vol. 208, p. 104452, 2021.
[16] H. Nohutcu, A. Demir, E. Ercan, E. Hokelekli, and G. Altintas, "Investigation of a historic masonry structure by numerical and operational modal analyses," Struct. Des. Tall Spec. Build., vol. 24, no. 13, pp. 821–834, 2015.
[17] A. Demir, H. Nohutcu, E. Ercan, E. Hokelekli, and G. Altintas, "Effect of model calibration on seismic behaviour of a historical mosque," Struct. Eng. Mech., vol. 60, no. 5, pp. 749–760, 2016.
[18] H. Sezen, R. Acar, A. Dogangun, and R. Livaoglu, "Dynamic analysis and seismic performance of reinforced concrete minarets," Eng. Struct., vol. 30, no. 8, pp. 2253–2264, 2008.
[19] A. Doğangün, R. Acar, R. Livaoğlu, and Ö. İ. Tuluk, "Performance of masonry minarets against earthquakes and winds in Turkey," in Proceedings of the 1st International Conference on Restoration of Heritage Masonry Structures, , pp. 24–27, April 2006.
[20] E. M. Higazy, "Vulnerability of historical minarets; investigation of their seismic assessment & retrofitting," Emir. J. Eng. Res., vol. 9, no. 2, pp. 59–64, 2004.
[21] A. G. El-Attar, A. M. Saleh, and A. H. Zaghw, "Conservation of a slender historical Mamluk-style minaret by passive control techniques," Struct. Control Health Monit. Off. J. Int. Assoc. Struct. Control Monit. Eur. Assoc. Control Struct., vol. 12, no. 2, pp. 157–177, 2005.
[22] A. Dogangun, R. Acar, H. Sezen, and R. Livaoglu, "Investigation of dynamic response of masonry minaret structures," Bull. Earthq. Eng., vol. 6, no. 3, pp. 505–517, 2008.
[23] A. Bayraktar, A. C. Altunişik, B. Sevim, and T. Türker, "Seismic response of a historical masonry minaret using a finite element model updated with operational modal testing," J. Vib. Control, vol. 17, no. 1, pp. 129–149, 2011.
[24] F. Portioli et al., "Seismic retrofitting of Mustafa Pasha Mosque in Skopje: finite element analysis," J. Earthq. Eng., vol. 15, no. 4, pp. 620–639, 2011.

[25] Y. Calayır, E. Sayın, and B. Yön, "Performance of structures in the rural area during the March 8, 2010 Elazığ-Kovancılar earthquake," Nat. Hazards, vol. 61, no. 2, pp. 703–717, 2012.
[26] A. Bayraktar, A. C. Altunişik, and M. Muvafik, "Damages of minarets during Erciş and Edremit earthquakes, 2011 in Turkey," 2014.
[27] M. Muvafik, "Field investigation and seismic analysis of a historical brick masonry minaret damaged during the Van Earthquakes in 2011," Earthq. Struct., vol. 6, no. 5, pp. 457–472, 2014.
[28] H. Nohutcu, E. Hokelekli, E. Ercan, A. Demir, and G. Altintas, "Collapse mechanism estimation of a historical slender minaret," Struct. Eng. Mech., vol. 64, no. 5, pp. 653–660, 2017.
[29] H. Nohutcu, "Seismic Failure Pattern Prediction in a Historical Masonry Minaret under Different Earthquakes," Adv. Civ. Eng., vol. 2019, 2019.
[30] A. Bayraktar and E. Hökelekli, "Influences of earthquake input models on nonlinear seismic performances of minaret-foundation-soil interaction systems," Soil Dyn. Earthq. Eng., vol. 139, p. 106368, 2020.
[31] T. Y. Altiok and A. Demir, "Collapse mechanism estimation of a historical masonry minaret considered soil-structure interaction," Earthq. Struct., vol. 21, no. 2, pp. 161–172, 2021.
[32] A. Demir and T. Y. Altıok, "Numerical assessment of a slender structure damaged during October 30, 2020, İzmir earthquake in Turkey," Bull. Earthq. Eng., pp. 1–26, 2021.
[33] T. Y. Altıok and A. Demir, "Seismic damage assessment of a historical masonry minaret considering soil-structure interaction," J. Struct. Eng. Appl. Mech., vol. 4, no. 3, pp. 196–212, Sep. 2021.
[34] E. Ercan, B. Arisoy, E. Hökelekli, and A. Nuhoğlu, "Estimation of seismic damage propagation in a historical masonry minaret," Sigma J. Eng. Nat. Sci. Ve Fen Bilim. Derg., vol. 35, no. 4, 2017.
[35] A. Bayraktar and E. Hökelekli, "Influences of earthquake input models on nonlinear seismic performances of minaret-foundation-soil interaction systems," Soil Dyn. Earthq. Eng., vol. 139, p. 106368, 2020.
[36] B. R. Hughes and S. A. A. Abdul Ghani, "A numerical investigation into the effect of windvent dampers on operating conditions," Build. Environ., vol. 44, no. 2, pp. 237–248, Feb. 2009.
[37] S. Liu, C. M. Mak, and J. Niu, "Numerical evaluation of louver configuration and ventilation strategies for the windcatcher system," Build. Environ., vol. 46, no. 8, pp. 1600–1616, Aug. 2011.
[38] H. Montazeri, "Experimental and numerical study on natural ventilation performance of various multi-opening wind catchers," Build. Environ., vol. 46, no. 2, pp. 370–378, Feb. 2011.
[39] B. R. Hughes, J. K. Calautit, and S. A. Ghani, "The development of commercial wind towers for natural ventilation: A review," Appl. Energy, vol. 92, pp. 606–627, Apr. 2012.
[40] O. Saadatian, L. C. Haw, K. Sopian, and M. Y. Sulaiman, "Review of windcatcher technologies," Renew. Sustain. Energy Rev., vol. 16, no. 3, pp. 1477–1495, Apr. 2012.
[41] B. M. Jones and R. Kirby, "Quantifying the performance of a top–down natural ventilation Windcatcher," Build. Environ., vol. 44, no. 9, pp. 1925–1934, Sep. 2009.
[42] A. A. Elmualim, "Effect of damper and heat source on wind catcher natural ventilation performance," Energy Build., vol. 38, no. 8, pp. 939–948, Aug. 2006.
[43] Y. Su, S. B. Riffat, Y.-L. Lin, and N. Khan, "Experimental and CFD study of ventilation flow rate of a Monodraught™ windcatcher," Energy Build., vol. 40, no. 6, pp. 1110–1116, Jan. 2008.
[44] A. Ural, A. Dogangun, and S. Meraki, "Response evaluation of historical crooked minaret under wind and earthquake loadings," Wind Struct., vol. 17, no. 3, pp. 345–359, 2013.
[45] A. Ural and F. K. Firat, "Evaluation of masonry minarets collapsed by a strong wind under uncertainty," Nat. Hazards, vol. 76, no. 2, pp. 999–1018, Mar. 2015.
[46] R. Reşatoğlu, T. Mirata, and L. Karaker, "Earthquake and wind load effects on existing RC minarets in north Cyprus," Int. J. Eng. Technol., vol. 7, no. 4, pp. 3074–3085, 2018.
[47] M. A. Adam, T. S. El-Salakawy, M. A. Salama, and A. A. Mohamed, "Assessment of structural condition of a historic masonry minaret in Egypt," Case Stud. Constr. Mater., vol. 13, p. e00409, Dec. 2020.
[48] E. Türkeli, "Dynamic Seismic and Wind Response of Masonry Minarets," Period. Polytech. Civ. Eng., vol. 64, no. 2, pp. 353–369, 2020.
[49] M. Pouraminian, "Multi-hazard reliability assessment of historical brick minarets," J. Build. Pathol. Rehabil., vol. 7, no. 1, p. 10, Dec. 2021.

[50] A. H. Al-Zuhairi, A. R. Ahmed, and S. R. Al-Zaidee, "Numerical Analysis of Historical Masonry Minaret Subjected to Wind Load," in Geotechnical Engineering and Sustainable Construction, M. O. Karkush and D. Choudhury, Eds., Singapore: Springer, pp. 545–555, 2022,.
[51] H. H. Awad and M. Desouki, "Integrating physical experiments with computational fluid dynamics to transform mosque minarets into efficient solar chimneys," Sci. Rep., vol. 14, no. 1, p. 9721, Apr. 2024.
[52] Turkish Standard Institute, Turkish Standard, TS498: The Calculation Values of Loads used in Designing Structural Elements, Ankara, Turkey, 1997.
[53] Dlubal Software, RWIND-Simulation Generation of WindInduced Loads on General Models: User Manual, October 2020. Available at: https://www.dlubal.com/en/downloads-and-information/documents/online-manuals/rwindsimulation-1/01/01.
[54] Dassault Systemes Simulia Corp., Abaqus v10, Providence, Rhode Island, USA, 2010.
[55] NTV Haber, http://arsiv.ntv.com.tr/news/120847.asp (accessed 29/10/2021).
[56] Hürriyet, http://www.hurriyetim.com.tr/haber/ (accessed 27/02/2002).
[57] Milliyet, "http://www.milliyet.com.tr/2003/02/09/guncel/gun15.html" (accessed 09/02/2003).
[58] Hürriyet, "http://www.hurriyetim.com.tr/haber/0" (accessed 24/07/2005).
[59] Haberler.com, "https://www.haberler.com/22-yillik-caminin-minaresi-yikildi-haberi/" (accessed 22/09/2019).
[60] Cumhuriyet, "http://www.cumhuriyet.com.tr" (accessed 10/04/2015).
[61] Haberler.com,"https://www.haberler.com/ordu-da-57-metrelik-minare-siddetli-ruzgarda-8074105-haberi/" (accessed 22/09/2019).
[62] Ajans Niğde, (2021). "http://www.ajansnigde.com/nigdede-cami-minaresi-yikildi_d89720.html" (erişim tarihi: 29/11/2021).
[63] Ankara Masası, (2021). "https://www.ankaramasasi.com/haber/1053206/aydinda-siddetli-ruzgar-minareyi-yikti-o-anlar-kamerada" (erişim tarihi: 29/11/2021).
[64] Türkiye Building Seismic Code-2018, Ankara, Türkiye.
[65] J. Lubliner, J. Oliver, S. Oller, and Ejij. Onate, 'A plastic-damage model for concrete', Int. J. Solids Struct., vol. 25, no. 3, pp. 299–326, 1989.
[66] J. Lee and G. L. Fenves, 'Plastic-damage model for cyclic loading of concrete structures', J. Eng. Mech., vol. 124, no. 8, pp. 892–900, 1998.
[67] M. Resta, A. Fiore, and P. Monaco, 'Non-linear finite element analysis of masonry towers by adopting the damage plasticity constitutive model', Adv. Struct. Eng., vol. 16, no. 5, pp. 791–803, 2013.
[68] M. Valente and G. Milani, 'Non-linear dynamic and static analyses on eight historical masonry towers in the North-East of Italy', Eng. Struct., vol. 114, pp. 241–270, 2016.
[69] M. Valente and G. Milani, 'Damage assessment and collapse investigation of three historical masonry palaces under seismic actions', Eng. Fail. Anal., vol. 98, pp. 10–37, 2019.
[70] E. Hökelekli and A. Al-Helwani, 'Effect of soil properties on the seismic damage assessment of historical masonry minaret–soil interaction systems', Struct. Des. Tall Spec. Build., vol. 29, no. 2, p. e1694, 2020.
[71] E. Hökelekli, A. Demir, E. Ercan, H. Nohutçu, and A. Karabulut, 'Seismic Assessment in a Historical Masonry Minaret by Linear and Non-linear Seismic Analyses', Period. Polytech. Civ. Eng., vol. 64, no. 2, pp. 438–448, 2020.
[72] T. Y. Altıok and A. Demir, 'Collapse mechanism estimation of a historical masonry minaret considered soil-structure interaction', Earthq. Struct., vol. 21, no. 2, pp. 161–172, 2021.
[73] R. Nayal and H. A. Rasheed, 'Tension stiffening model for concrete beams reinforced with steel and FRP bars', J. Mater. Civ. Eng., vol. 18, no. 6, pp. 831–841, 2006.
[74] B. Wahalathantri, D. Thambiratnam, T. Chan, and S. Fawzia, 'A material model for flexural crack simulation in reinforced concrete elements using ABAQUS', in Proceedings of the first international conference on engineering, designing and developing the built environment for sustainable wellbeing, Queensland University of Technology, pp. 260–264, 2011.
[75] R. I. Gilbert and R. F. Warner, 'Tension stiffening in reinforced concrete slabs', J. Struct. Div., vol. 104, no. 12, pp. 1885–1900, 1978.
[76] A. S. Genikomsou and M. A. Polak, 'Finite element analysis of punching shear of concrete slabs using damaged plasticity model in ABAQUS', Eng. Struct., vol. 98, pp. 38–48, 2015.

[77] Italian Public Works Council. (2019). "Guidelines for Application of Italian Building Code; Istituto Poligrafico e Zecca dello Stato", Roma, Italy.
[78] Eurocode 8. (2005). "Design of Structures for Earthquake Resistance—Part 3: Assessment and Retrofitting of Buildings". CEN: Brussels, Belgium.
[79] A. Demir and T. Y. Altıok, 'Numerical assessment of a slender structure damaged during October 30, 2020, İzmir earthquake in Turkey', Bull. Earthq. Eng., vol. 19, no. 14, pp. 5871–5896, 2021.
[80] T. Y. Altıok and A. Demir, 'Seismic damage assessment of a historical masonry minaret considering soil-structure interaction', J. Struct. Eng. Appl. Mech., vol. 4, no. 3, pp. 196–212, Sep. 2021.